

## COMMUNICATION

# Formation of a Stable Oligomer of $\beta$ -2 Microglobulin Requires only Transient Encounter with Cu(II)

Matthew F. Calabrese and Andrew D. Miranker\*

Department of Molecular  
Biophysics and Biochemistry  
Yale University, 260 Whitney  
Avenue, New Haven  
CT 06520-8114, USA

$\beta$ -2 Microglobulin ( $\beta$ 2m) is a small, globular protein, with high solubility under conditions comparable to human serum. A complication of hemodialysis in renal failure patients is the deposition of unmodified  $\beta$ 2m as amyloid fibers. *In vitro*, exposure of  $\beta$ 2m to equimolar  $\text{Cu}^{2+}$  under near-physiological conditions can result in self-association leading to amyloid fiber formation. Previously, we have shown that the early steps in this process involve a catalyzed structural rearrangement followed by formation of discrete oligomers. These oligomers, however, have a continued requirement for  $\text{Cu}^{2+}$  while mature fibers are resistant to addition of metal chelate. Here, we report that the transition from  $\text{Cu}^{2+}$  dependent to chelate resistant states occurs in the context of small oligomers, dimeric to hexameric in size. These species require  $\text{Cu}^{2+}$  to form, but once generated, do not need metal cation for stability. Importantly, this transition occurs gradually over several days and the resulting oligomers are isolatable and kinetically stable on timescales exceeding weeks. In addition, formation is enhanced by levels of urea similar to those found in hemodialysis patients. Our results are consistent with our hypothesis that transient encounter of full-length wild-type  $\beta$ 2m with transition metal cation at the dialysis membrane interface is causal to dialysis related amyloidosis.

© 2007 Published by Elsevier Ltd.

\*Corresponding author

**Keywords:**  $\beta$ -2 microglobulin; amyloid; copper; dialysis; aggregation

Under normal conditions *in vivo*, proteins possess functions, which are dictated, in part, by their unique native fold. In the clinical amyloidoses, changes in native structure or in the folding pathway leading to this structure initiate pathological aggregation.<sup>1</sup> In many cases, this change is due to mutation or covalent modification of the precursor protein resulting in an increase in amyloidogenic propensity. This is the case in Huntington's disease<sup>2</sup> and light chain amyloidosis.<sup>3,4</sup> and may also play a role in the progression of Alzheimer's disease.<sup>5</sup> Unmodified proteins can also give rise to amyloid as a result of changes in the protein environment. This is observed in type II diabetes<sup>6,7</sup> and dialysis related amyloidosis

(DRA).<sup>8,9</sup> DRA is a debilitating complication of long-term hemodialysis. It is characterized by gradual accumulation of fibrous deposits consisting primarily of  $\beta$ -2 microglobulin ( $\beta$ 2m).<sup>10</sup> Previously, we have shown that unmodified  $\beta$ 2m spontaneously aggregates upon incubation with stoichiometric  $\text{Cu}^{2+}$  under solution conditions comparable to human serum.<sup>8,11</sup> Indeed, metal cations appear to be of general importance to amyloid formation with interactions reported for PrP in Creutzfeldt-Jakob disease,<sup>12,13</sup>  $\alpha$ -synuclein in Parkinson's disease,<sup>14,15</sup> and  $\text{A}\beta$  in Alzheimer's disease.<sup>16,17</sup>

$\beta$ 2m is the 12 kDa, globular light chain component of the class I major histocompatibility complex.<sup>18</sup> Its topology is a seven-stranded  $\beta$ -sandwich stabilized, in part, by a disulfide bond bridging the sandwich. As part of normal turnover,  $\beta$ 2m is released to the serum where it is subsequently degraded by the kidneys. In patients with end stage renal disease who are on long-term hemodialysis therapy,  $\beta$ 2m is not efficiently cleared. Serum levels can increase from  $\sim 0.1 \mu\text{M}$  to  $>5 \mu\text{M}$ , and fibrous plaques composed

Abbreviations used:  $\beta$ 2m,  $\beta$ -2 microglobulin; DRA, dialysis related amyloidosis; SEC, size-exclusion chromatography; AUC, analytical ultracentrifugation; EPR, electron paramagnetic resonance.

E-mail address of the corresponding author:  
[andrew.miranker@yale.edu](mailto:andrew.miranker@yale.edu)

primarily of unmodified  $\beta 2m$  are detected principally in the joint spaces.<sup>10,19</sup>

An increase in the serum concentration may be necessary, but is not sufficient to induce DRA. In other clinical conditions, such as hepatitis C and chronic leukemia,  $\beta 2m$  levels are elevated, yet no amyloid deposits are observed.<sup>20,21</sup> Additionally, *in vitro*,  $\beta 2m$  is stable and monomeric under near-physiological conditions at concentrations over 1000-fold those found *in vivo*.<sup>22</sup> We have previously reported that stoichiometric levels of  $Cu^{2+}$  can induce oligomerization and aggregation of  $\beta 2m$  *in vitro* under conditions comparable with human serum.<sup>8,23</sup> These oligomers form over  $\sim 1$  h time period and are absolutely dependent on the presence of metal for stability. In marked contrast, mature fibers require weeks for significant accumulation and remain stable even upon addition of metal chelate. This generates a puzzle in which the complete role of metal is uncertain. Importantly, it is unclear whether  $Cu^{2+}$  is consumed in the reaction becoming an integral part of the aggregate. Alternatively, it may serve as a catalyst enabling access to a novel state. This may have clinical relevance as  $\beta 2m$  likely only experiences transient exposure to free  $Cu^{2+}$  during dialysis therapy.

For  $\beta 2m$ ,  $Cu^{2+}$  serves two critical roles in initiating aggregation. First,  $Cu^{2+}$  bound to native monomeric  $\beta 2m$  catalyzes a molecular rearrangement to a state we have termed  $M^*$ . This state is native-like by near-UV circular dichroism and proton NMR.<sup>24</sup> The atomic structure of a mutant analogue of  $M^*$  reveals the loss of a  $\beta$ -bulge in an edge strand, and exhibits partial repacking of the hydrophobic core.<sup>23,24</sup> This structural reorganization is facilitated by the isomerization of a conserved *cis*-proline at the  $Cu^{2+}$  binding site. Indeed, the mutation of this *cis*-peptide to a non-prolyl amino acid (P32A) results in an increase of the  $Cu^{2+}$  affinity from  $\sim 3 \mu M$  to  $\sim 0.5$  nM. This suggests that binding energy is used to drive the conformational change. These changes appear necessary, but are not sufficient for aggregation. For example, the related mutant P32G has been shown to elongate fibers prepared *de novo* at pH 2.5 and subsequently stabilized using serum components at pH 7.0.<sup>25</sup> In our hands, the P32A mutant mimics the  $M^*$  state, but still requires metal to stabilize oligomerization.  $Cu^{2+}$  is therefore playing a structural role in oligomer assembly.<sup>23</sup> Both  $M^*$  and its oligomers differ from mature amyloid in that the former are reversible in response to addition of chelate. The nature of the transition between these oligomers and amyloid is therefore unknown.

### Cu(II) induced assembly of chelate resistant states

Amyloid formation by  $\beta 2m$  involves changes in conformation, oligomeric size, and sensitivity to chelate. To study intermediates of this process, near-physiological solution conditions have been chosen which allow fiber formation to occur on a timescale of several weeks.<sup>23</sup> We have previously shown that

oligomerization can be followed by NMR, ultracentrifugation, size-exclusion chromatography (SEC), and fluorescence.<sup>23</sup> Here, we monitor oligomerization using SEC in order to follow the kinetics and size of oligomeric states. This is achieved by adding EDTA to aliquots of a standard amyloid formation reaction. The distribution of aggregates at discrete time points is then evaluated.

The first states insensitive to chelate are small and soluble (Figure 1). After  $\sim 2$  h of incubation with  $Cu^{2+}$ , approximately half the total protein is present in oligomeric states (Figure 1(a)). These have previously been assigned to dimers, tetramers, and hexamers using sedimentation velocity analytical ultracentrifugation (AUC).<sup>23</sup> Addition of 10 mM EDTA at this time point causes all oligomers to revert to monomer (Figure 1(b)) yielding a spectrum

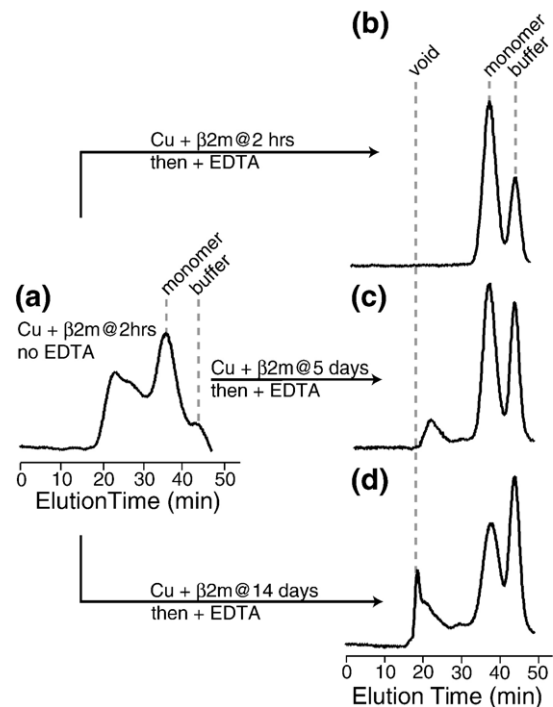


**Figure 1.** Aggregate formation before and after removal of  $Cu^{2+}$ . (a) 100  $\mu M$   $\beta 2m$  incubated with 200  $\mu M$   $Cu^{2+}$  for 2 h and run over a sizing column equilibrated with  $Cu^{2+}$ . (b), (c) and (d) Alternatively, a sample incubated with  $Cu^{2+}$  for 2 h, 5 days, and 14 days, respectively, were quenched with 10 mM EDTA. Fractionation on the same column equilibrated with EDTA is shown. The label *void* denotes the void volume, *monomer* denotes the elution point of monomeric  $\beta 2m$ , and *buffer* denotes the elution point of small molecule buffer components (e.g.  $Cu^{2+}$ , EDTA). SEC was conducted using a 10/300 mm column, with a 25 ml bed volume of Superdex 75. Sample volumes ranging from 70  $\mu l$ –150  $\mu l$  were studied. For analysis of chelate-resistant states, reaction aliquots were removed and EDTA added to 10 mM. This was then incubated at 37  $^{\circ}C$  for  $\sim 20$  min before analysis. Column calibration was performed using aprotinin, cytochrome *c*, carbonic anhydrase, and albumin (6.5–66 kDa). Human-derived  $\beta 2m$  was purified as described.<sup>8</sup> Unless stated otherwise all reactions were in 200 mM potassium acetate, 500 mM urea, 25 mM Mops (pH 7.4) at 37  $^{\circ}C$ .

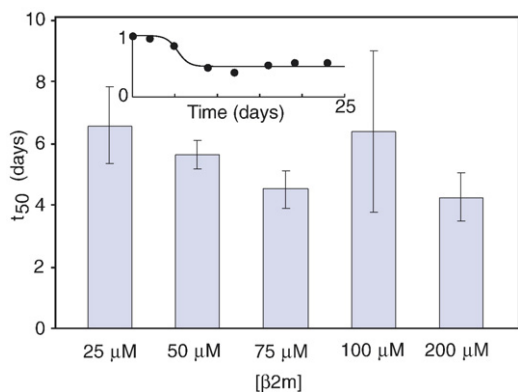


**Figure 2.** Kinetics of chelate resistance shows no concentration dependence. For each stated concentration of protein, a parent reaction was initiated at a stoichiometry of 2:1,  $\text{Cu}^{2+}$ :  $\beta 2m$ , split into aliquots, and incubated at 37 °C. At discrete time points, EDTA was added to an aliquot to 10 mM and analyzed by SEC. Inset: A representative time course and fit of 100  $\mu\text{M}$   $\beta 2m$ , 200  $\mu\text{M}$   $\text{Cu}^{2+}$ , and 500 mM urea. The  $y$ -axis represents the fraction of chelate-sensitive material (the proportion of material that reverts to monomer upon EDTA addition). SEC chromatographs were integrated using the Curve Fitting Toolbox in MATLAB V 7.2.0.232 (The MathWorks Inc.). For kinetics, three-week time courses were fit to:  $y = p / (1 + e^{-(t-t_{50})/\tau})$ . Where  $p$  is plateau height,  $t_{50}$  is the midpoint of the transition, and  $\tau$  reflects the curvature.  $y$  is the normalized fraction of protein in a chelate-resistant state. In all analyses, error bars represent  $\pm 1$  standard deviation derived from  $\geq 3$  data sets.

indistinguishable from  $\beta 2m$  incubated in the absence of metal (not shown). In contrast, the addition of EDTA to the same reaction after two weeks of incubation is not fully reversible (Figure 1(d)). Aggregates are apparent and elute in the void volume of the column. For the SEC matrix used here, the void volume represents states larger than  $\sim 70$  kDa in size. Surprisingly, large aggregates are not the first states to demonstrate chelate resistance. Addition of EDTA after five days incubation results in a persistent oligomeric population (Figure 1(c)). As with the void volume fraction, these states give enhanced fluorescence upon binding the amyloid histological dye Thioflavin T<sup>26</sup> (data not shown). Furthermore, the oligomeric nature of this fraction was confirmed by sedimentation velocity AUC (not shown). Upon comparison of the elution times of these oligomers to known standards, we assess the first EDTA resistant states to be dimeric to tetrameric in size, similar to the size-distribution of the chelate sensitive states populated on the hour time scale.<sup>23</sup>

Conformational changes and not collisional encounter limit the rate of forming chelate resistant states. To gain mechanistic insight into the nature of the limiting step for attaining chelate resistance, kinetics were carried out monitored by SEC. At discrete time points, an aliquot of a parent reaction (100  $\mu\text{M}$   $\beta 2m$ , 200  $\mu\text{M}$   $\text{Cu}^{2+}$ , 500 mM urea) was removed, and the relative fraction of chelate-resistant oligomers was determined. The resulting

plot yields a midpoint time to conversion ( $t_{50}$ ) of  $\sim$ one week (Figure 2, inset). The non-exponential nature of the kinetics is reminiscent of nucleation generally associated with fiber formation. Here, however, it may simply reflect the presence of an additional intervening intermediate. This assay was repeated over a series of concentrations of  $\beta 2m$  (Figure 2). For all concentrations, the  $t_{50}$  values lie within a twofold range and are within error, suggestive of an intervening intermediate. Irrespective of mechanism, the concentration independence makes plain that formation of chelate-resistant states is rate-limited by rearrangement rather than by oligomerization.

Local, not global rearrangements facilitate the transition to chelate resistance. Reactions of 100  $\mu\text{M}$   $\beta 2m$  were allowed to incubate with 200  $\mu\text{M}$   $\text{Cu}^{2+}$  at various concentrations of urea for  $\sim 12$  days before EDTA was added (Figure 3(a)). The resulting SEC plots show that for 0, 100, 250, and 500 mM urea,

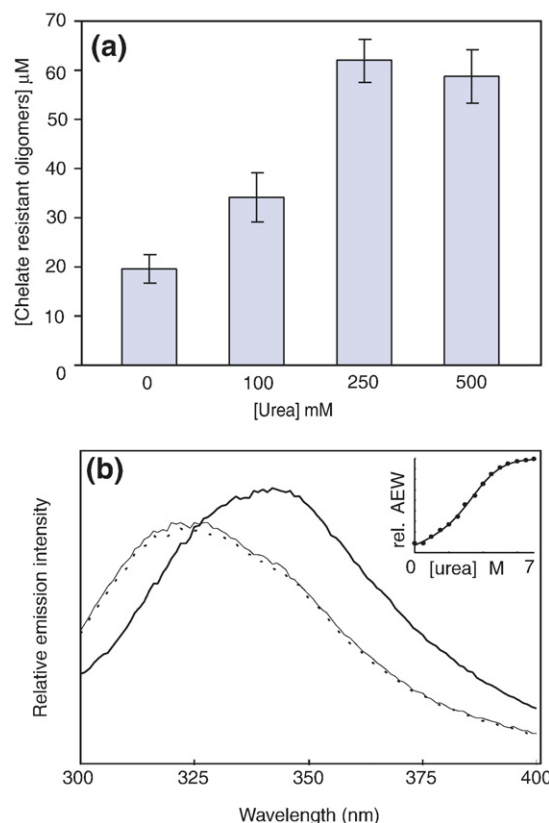


**Figure 3.** Formation of chelate-resistant states is enhanced by sub-denaturing levels of urea (a) For each stated urea concentration, a reaction at 100  $\mu\text{M}$  protein and 200  $\mu\text{M}$   $\text{Cu}^{2+}$  was initiated. After 12 days of incubation, EDTA was added to 10 mM and analysis performed by SEC. The  $y$ -axis refers to [chelate resistant oligomers] in monomer units. (b) Intrinsic fluorescence of  $\beta 2m$  in the presence of 0 (dotted line), 500 mM (thin continuous line), and 7 M (thick continuous line) urea. Samples are at 2.5  $\mu\text{M}$   $\beta 2m$  and 30  $\mu\text{M}$   $\text{Cu}^{2+}$  to ensure  $>90\%$  of signal is from holo- $\beta 2m$ .<sup>47</sup> Inset: Urea denaturation of  $\beta 2m + \text{Cu}^{2+}$  at 37 °C monitored by intrinsic average emission wavelength as described.<sup>8,47</sup>

19.5( $\pm 3$ )  $\mu M$ , 34( $\pm 5$ )  $\mu M$ , 62( $\pm 4$ )  $\mu M$ , and 59( $\pm 5$ )  $\mu M$   $\beta 2m$  (in monomeric units) is in chelate resistant states, respectively. Although chelate-resistant states develop in the absence of denaturants, formation is plainly sensitive to low concentrations of urea. This may have clinical relevance as end stage renal disease patients are uremic with serum urea levels exceeding 50 mM.<sup>27–29</sup> The enhancement due to urea appears maximal at a concentration of 250 mM, since inclusion of additional urea up to 500 mM has no further effect on the extent of aggregation. Note, 500 mM urea is well below the global unfolding transition (3.8 M) (Figure 3(b), inset). Furthermore, this level of urea does not compromise the global fold of  $\beta 2m$  as evidenced by intrinsic fluorescence (Figure 3(b)) and circular dichroism (CD) (not shown). Similarly, we have previously reported no alteration in near-UV CD between apo- and holo- $\beta 2m$  under conditions identical to those used here.<sup>23</sup> The progression of amyloid formation under near-native solution conditions combined with the observed lack of concentration dependence on reaction kinetics suggest that formation of chelate-resistant oligomers involves rearrangement within native-like precursors. We note that at pH 3.6 where the core of  $\beta 2m$  remains intact but the edge strands are perturbed, amyloid formation by  $\beta 2m$  occurs spontaneously.<sup>30,31</sup> Additionally, if physiological conditions are preserved but edge strands are mutated or truncated, amyloid formation also proceeds from a partially structured state.<sup>32,33</sup> Taken together, these data suggest that for wild-type protein under native conditions, local rearrangements trigger aggregation of  $\beta 2m$ . Indeed, the possibility that native-like protein can participate in aggregation has been suggested in amyloid formation of acylphosphatase,<sup>34</sup> ribonuclease A,<sup>35</sup> and cystatin.<sup>36,37</sup>

### Mechanism of stabilization

Chelate-resistant oligomers do not readily dissociate. To assess this, a parent amyloid reaction of  $\beta 2m$  was incubated with  $Cu^{2+}$  in the absence of urea for  $\sim 12$  days. EDTA was then added to the whole reaction and an aliquot removed and immediately analyzed by SEC (Figure 4(a)). Under these conditions, 17( $\pm 1.5$ )% of the protein is in the oligomeric fraction. The remainder of the reaction was allowed to continue incubating at 37 °C before analysis. Remarkably, after five and 17 days of incubation in the presence of EDTA, 15.3( $\pm 2.7$ )% and 18.7( $\pm 0.8$ )% of the protein remains in the oligomeric fraction, i.e. there is no apparent dissociation on the timescale of weeks. In addition, fractions corresponding only to the oligomeric states can be pooled and rerun over the same sizing column (Figure 4(b) and (c)). No dissociation to monomer is apparent by this procedure. Quantitation using reverse-phase HPLC and analysis with mass spectrometry reveal that these oligomers are not cross-linked and are composed of full-length, unmodified, wild-type  $\beta 2m$  (data not shown). This suggests that the oligomers are

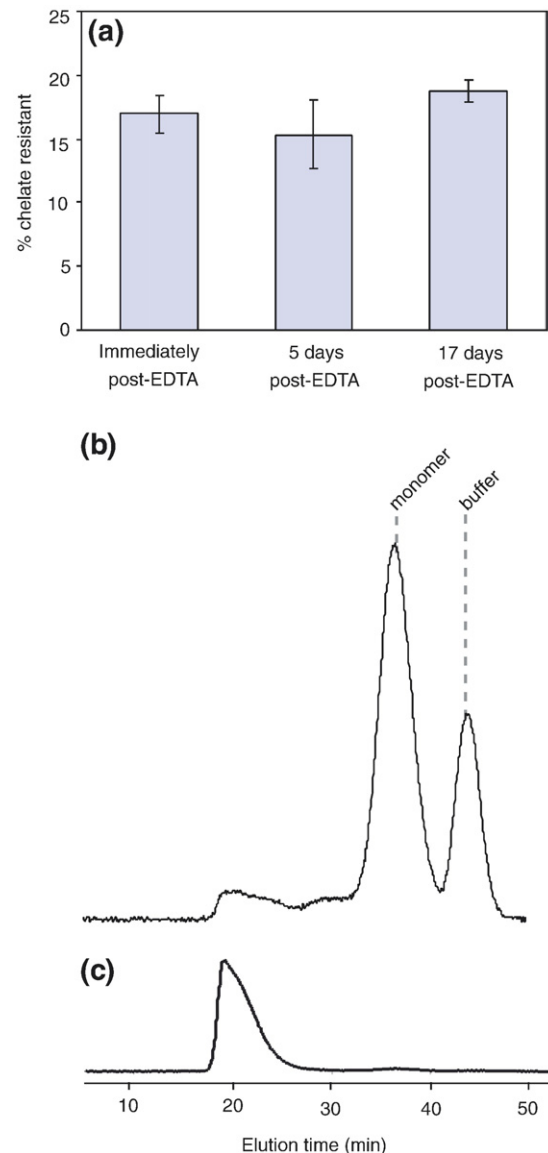


**Figure 4.** Chelate-resistant oligomers are kinetically stable. (a) A parent reaction was initiated with 100  $\mu M$   $\beta 2m$ , 200  $\mu M$   $Cu^{2+}$  in the absence of urea and allowed to incubate for 12 days at 37 °C. The reaction was then quenched with EDTA to 10 mM and split into three aliquots. Aliquots were then analyzed either immediately by SEC or were left to incubate at 37 °C for 5 and 17 days before analysis. (b) A reaction of  $\beta 2m + Cu^{2+}$  was allowed to incubate at 37 °C for 12 days in the absence of urea and was then quenched with EDTA. (c) Selected fractions of chelate-resistant oligomers (principally corresponding to the states eluting near 20 min) were pooled, concentrated, and rerun over the same size-exclusion column. Note, (b) and (c) were scaled independently.

kinetically stable states. The observation of slowly forming, isolatable, robust oligomers preceding fiber formation is not unique to  $\beta 2m$ . For example, stable dimers and tetramers of cystatin have also been reported under non-denaturing conditions.<sup>36,37</sup>

Chelate resistance corresponds to a loss of cation dependence. The presence of  $Cu^{2+}$  bound to  $\beta 2m$  was assessed using electron paramagnetic resonance

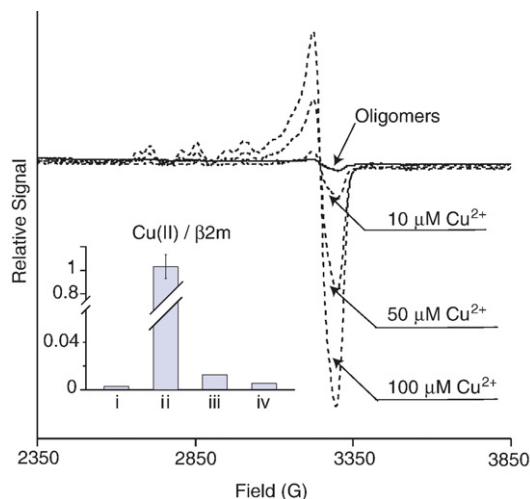


**Figure 5.** Chelate-resistant oligomers have no  $\text{Cu}^{2+}$  present. (a) Shown is a representative EPR spectrum of SEC purified chelate-resistant oligomers at  $80 \mu\text{M}$  (continuous line). For comparison, copper acetate standards at  $100$ ,  $50$ , and  $10 \mu\text{M}$  are shown. Integration of the oligomer spectrum shown yields a  $[\text{Cu}^{2+}] < 3 \mu\text{M}$ . Inset: Molar ratio of  $\text{Cu}^{2+} : \beta 2m$  are shown for the following samples: i,  $\beta 2m$  in the absence of  $\text{Cu}^{2+}$  (negative control); ii,  $\beta 2m$  incubated with  $\text{Cu}^{2+}$  for  $\sim 2$  h (Figure 1(a)) before exchange into a metal and chelate-free buffer; iii, chelate-resistant oligomers purified from both monomer and free  $\text{Cu}^{2+}$  by SEC (above, continuous line); iv, mature aggregates which were washed of free metal by repeated centrifugation and resuspension using buffer containing  $10 \text{ mM}$  EDTA. Note, error bars are not shown for mole ratios, which reflect  $\text{Cu}^{2+}$  levels below the detection limit. EPR measurements were conducted on a Bruker Instruments (Billerica MA) Elexsys EPR spectrometer operated at  $20 \text{ K}$ . Samples were  $150\text{--}200 \mu\text{l}$  with  $30\%$  ethylene glycol as a cryoprotectant.  $\text{Cu}^{2+}$  concentrations were determined by double integration of EPR spectra.

spectroscopy (EPR) after separating protein from free  $\text{Cu}^{2+}$ . Briefly, oligomers were purified from both monomer and free  $\text{Cu}^{2+}$  by SEC using a run buffer containing  $10 \text{ mM}$  EDTA. Remarkably, purified oligomers do not yield a detectable EPR absorption peak for  $\text{Cu}^{2+}$  (Figure 5 (and inset)). Similarly, mature aggregates were prepared and washed of free  $\text{Cu}^{2+}$  by repeated centrifugation and resuspension. These too reveal no apparent bound  $\text{Cu}^{2+}$ . To ensure that aggregates are not EPR silent due to formation of a diamagnetic complex, chelate-resistant oligomers were denatured in  $7 \text{ M}$  guanadine HCl and analyzed yielding qualitatively similar results (data not shown). Standards were used to establish an upper limit on the order of  $0.03$  for the molar ratio of  $\text{Cu}^{2+} : \beta 2m$  in oligomers and  $0.01$  in mature aggregates. As a control,  $\beta 2m$  incubated with  $\text{Cu}^{2+}$  for  $2 \text{ h}$  before chelate-free removal of unbound metal shows  $\sim 1:1$  cation binding (Figure 5 (inset)).

Progress has been made at determining a subset of the structural consequences of  $\text{Cu}^{2+}$  binding to monomeric  $\beta 2m$ .<sup>24,38</sup> Briefly, we have proposed that  $\text{Cu}^{2+}$  acts to catalyze the isomerization of a conserved *cis*-proline (P32) leading to an activated

monomeric state,  $M^*$ .<sup>24</sup> Intriguingly, this state may be similar to a refolding intermediate identified by others.<sup>25,39,40</sup> The changes evident in our atomic model of a mutant analogue of  $M^*$ , P32A, are necessary to induce amyloid formation, but are not sufficient. For example, at low concentration, P32A remains monomeric in the absence of metal. Importantly, this mutant has a  $\sim 10,000$  fold increase in affinity for  $\text{Cu}^{2+}$  compared to wild-type. This highlights an additional role for metal, namely as a tether between multiple  $M^*$  states.<sup>23,24</sup> Indeed, this may be approximated at high concentrations where the apo-P32A structure reveals a dimer whose interface includes four possible coordinating histidine residues which reside in close proximity across an acidic cleft. After oligomers have formed, conversion to chelate-resistant states occurs slowly and is accelerated with urea. This suggests that the transition from chelate-sensitive to chelate-resistant oligomers requires interaction between rarely populated conformers. In the absence of tethering, such a process would rarely occur, as it is dependent on collision.<sup>41</sup> The observed lack of concentration dependence on the rate of formation of  $\text{Cu}^{2+}$ -free oligomers is therefore consistent with tethering. Such a mechanism would greatly increase the productive encounter of high-energy states by raising the local protein concentration.

Structural modulations by transition metals are deeply rooted in biology. Metal binding has been observed to induce folding in unstructured regions of both proteins and nucleic acids.<sup>42,43</sup> A canonical example is the zinc-finger motif where a fold lacking a well-defined hydrophobic core can be stabilized by specific metal coordination.<sup>44</sup> Metals can also catalyze isomerization of the peptide backbone<sup>45</sup> or tether adjacent subunits within a complex as a shared ligand.<sup>46</sup> These functional roles for metals, together with their clear role in pathology, demonstrate the tremendous importance of understanding the changes that can be induced and regulated by metal cations. Therefore, the sequence of changes for  $\beta 2m$ , including binding, catalyzed conformational change, tethering, and release, may be an embodiment of general rules applicable across structural biology.

## Acknowledgements

We thank Dr A. Valentine, C.M. Eakin, and D. Blaho for helpful discussions. We thank Professor G. Brudvig, J. McEvoy, G. Ulas, and C. Cady for assistance with EPR spectroscopy, and A. Ruschak for assistance with data analysis. We are also grateful to C.M. Eakin for careful reading of the manuscript. This work was supported by the US National Institutes of Health (DK54899). The authors declare that they have no competing financial interests.

## Supplementary Data

Supplementary data associated with this article can be found, in the online version, at [doi:10.1016/j.jmb.2006.12.034](https://doi.org/10.1016/j.jmb.2006.12.034)

## References

- Kelly, J. W. (1998). The alternative conformations of amyloidogenic proteins and their multi-step assembly pathways. *Curr. Opin. Struct. Biol.* **8**, 101–106.
- Scherzinger, E., Sittler, A., Schweiger, K., Heiser, V., Lurz, R., Hasenbank, R. *et al.* (1999). Self-assembly of polyglutamine-containing huntingtin fragments into amyloid-like fibrils: implications for Huntington's disease pathology. *Proc. Natl Acad. Sci. USA*, **96**, 4604–4609.
- Davis, D. P., Gallo, G., Vogen, S. M., Dul, J. L., Sciarretta, K. L., Kumar, A. *et al.* (2001). Both the environment and somatic mutations govern the aggregation pathway of pathogenic immunoglobulin light chain. *J. Mol. Biol.* **313**, 1021–1034.
- Bellotti, V., Mangione, P. & Merlini, G. (2000). Review: immunoglobulin light chain amyloidosis—the archetype of structural and pathogenic variability. *J. Struct. Biol.* **130**, 280–289.
- Zhang, Q., Powers, E. T., Nieva, J., Huff, M. E., Dendle, M. A., Bieschke, J. *et al.* (2004). Metabolite-initiated protein misfolding may trigger Alzheimer's disease. *Proc. Natl Acad. Sci. USA*, **101**, 4752–4757.
- Hull, R. L., Westermark, G. T., Westermark, P. & Kahn, S. E. (2004). Islet amyloid: a critical entity in the pathogenesis of type 2 diabetes. *J. Clin. Endocrinol. Metab.* **89**, 3629–3643.
- Kahn, S. E., Andrikopoulos, S. & Verchere, C. B. (1999). Islet amyloid: a long-recognized but underappreciated pathological feature of type 2 diabetes. *Diabetes*, **48**, 241–253.
- Morgan, C. J., Gelfand, M., Atreya, C. & Miranker, A. D. (2001). Kidney dialysis-associated amyloidosis: a molecular role for copper in fiber formation. *J. Mol. Biol.* **309**, 339–345.
- Gejyo, F., Yamada, T., Odani, S., Nakagawa, Y., Arakawa, M., Kunitomo, T. *et al.* (1985). A new form of amyloid protein associated with chronic hemodialysis was identified as beta 2-microglobulin. *Biochem. Biophys. Res. Commun.* **129**, 701–706.
- Floege, J. & Ehlerting, G. (1996). Beta-2-microglobulin-associated amyloidosis. *Nephron*, **72**, 9–26.
- Eakin, C. M. & Miranker, A. D. (2005). From chance to frequent encounters: origins of beta2-microglobulin fibrillogenesis. *Biochim. Biophys. Acta*, **1753**, 92–99.
- Jobling, M. F., Huang, X., Stewart, L. R., Barnham, K. J., Curtain, C., Volitakis, I. *et al.* (2001). Copper and zinc binding modulates the aggregation and neurotoxic properties of the prion peptide PrP106-126. *Biochemistry*, **40**, 8073–8084.
- Wadsworth, J. D., Hill, A. F., Joiner, S., Jackson, G. S., Clarke, A. R. & Collinge, J. (1999). Strain-specific prion-protein conformation determined by metal ions. *Nature Cell Bio.* **1**, 55–59.
- Uversky, V. N., Li, J. & Fink, A. L. (2001). Metal-triggered structural transformations, aggregation, and fibrillation of human alpha-synuclein. A possible molecular link between Parkinson's disease and heavy metal exposure. *J. Biol. Chem.* **276**, 44284–44296.
- Rasia, R. M., Bertoncini, C. W., Marsh, D., Hoyer, W., Cherny, D., Zweckstetter, M. *et al.* (2005). Structural characterization of copper(II) binding to alpha-synuclein: Insights into the bioinorganic chemistry of Parkinson's disease. *Proc. Natl Acad. Sci. USA*, **102**, 4294–4299.
- Miura, T., Suzuki, K., Kohata, N. & Takeuchi, H. (2000). Metal binding modes of Alzheimer's amyloid beta-peptide in insoluble aggregates and soluble complexes. *Biochemistry*, **39**, 7024–7031.
- Bush, A. I. & Tanzi, R. E. (2002). The galvanization of beta-amyloid in Alzheimer's disease. *Proc. Natl Acad. Sci. USA*, **99**, 7317–7319.
- Bjorkman, P. J., Saper, M. A., Samraoui, B., Bennett, W. S., Strominger, J. L. & Wiley, D. C. (1987). Structure of the human class I histocompatibility antigen, HLA-A2. *Nature*, **329**, 506–512.
- Bellotti, V., Stoppini, M., Mangione, P., Sunde, M., Robinson, C., Asti, L. *et al.* (1998). Beta-2-microglobulin can be refolded into a native state from ex vivo amyloid fibrils. *Eur. J. Biochem.* **258**, 61–67.
- Malaguarnera, M., Restuccia, S., Di Fazio, I., Zoccolo, A. M., Trovato, B. A. & Pistone, G. (1997). Serum beta-2-microglobulin in chronic hepatitis C. *Dig. Dis. Sci.* **42**, 762–776.
- Keating, M. J. (1999). Chronic lymphocytic leukemia. *Semin. Oncol.* **26**, 107–114.
- Okon, M., Bray, P. & Vucelic, D. (1992). <sup>1</sup>H NMR assignments and secondary structure of human beta 2-microglobulin in solution. *Biochemistry*, **31**, 8906–89015.
- Eakin, C. M., Attenello, F. J., Morgan, C. J. & Miranker, A. D. (2004). Oligomeric assembly of native-like precursors precedes amyloid formation by beta-2 microglobulin. *Biochemistry*, **43**, 7808–7815.
- Eakin, C. M., Berman, A. J. & Miranker, A. D. (2006). A native to amyloidogenic transition regulated by a backbone trigger. *Nature Struct. Mol. Biol.* **13**, 202–208.
- Jahn, T. R., Parker, M. J., Homans, S. W. & Radford, S. E. (2006). Amyloid formation under physiological conditions proceeds via a native-like folding intermediate. *Nature Struct. Mol. Biol.* **13**, 195–201.
- LeVine, H., 3rd (1993). Thioflavine T interaction with synthetic Alzheimer's disease beta-amyloid peptides: detection of amyloid aggregation in solution. *Protein Sci.* **2**, 404–410.
- Cheng, M. F., Liu, H. L., Wu, A. B., Hsieh, R. Y., Guo, H. R. & Huang, J. J. (2006). Clinical characteristics and outcomes of new uremic patients with extreme azotemia in southern Taiwan. *Hemodial. Int.* **10**, 294–302.
- Kassirer, J. (1971). Clinical evaluation of kidney function: glomerular function. *N. Engl. J. Med.* **285**, 385–389.
- Dember, L. M. & Jaber, B. L. (2006). Dialysis-related amyloidosis: late finding or hidden epidemic? *Semin. Dial.* **19**, 105–109.
- Hoshino, M., Katou, H., Hagihara, Y., Hasegawa, K., Naiki, H. & Goto, Y. (2002). Mapping the core of the beta(2)-microglobulin amyloid fibril by H/D exchange. *Nature Struct. Biol.* **9**, 332–336.
- McParland, V. J., Kalverda, A. P., Homans, S. W. & Radford, S. E. (2002). Structural properties of an amyloid precursor of beta(2)-microglobulin. *Nature Struct. Biol.* **9**, 326–331.
- Jones, S., Smith, D. P. & Radford, S. E. (2003). Role of the N and C-terminal strands of beta 2-microglobulin in amyloid formation at neutral pH. *J. Mol. Biol.* **330**, 935–941.
- Esposito, G., Michelutti, R., Verdonesi, G., Viglino, P.,

- Hernandez, H., Robinson, C. V. *et al.* (2000). Removal of the N-terminal hexapeptide from human beta2-microglobulin facilitates protein aggregation and fibril formation. *Protein Sci.* **9**, 831–845.
34. Plakoutsi, G., Taddei, N., Stefani, M. & Chiti, F. (2004). Aggregation of the Acylphosphatase from *Sulfolobus solfataricus*: the folded and partially unfolded states can both be precursors for amyloid formation. *J. Biol. Chem.* **279**, 14111–14119.
  35. Sambashivan, S., Liu, Y., Sawaya, M. R., Gingery, M. & Eisenberg, D. (2005). Amyloid-like fibrils of ribonuclease A with three-dimensional domain-swapped and native-like structure. *Nature*, **437**, 266–269.
  36. Sanders, A., Jeremy Craven, C., Higgins, L. D., Giannini, S., Conroy, M. J., Hounslow, A. M. *et al.* (2004). Cystatin forms a tetramer through structural rearrangement of domain-swapped dimers prior to amyloidogenesis. *J. Mol. Biol.* **336**, 165–178.
  37. Staniforth, R. A., Giannini, S., Higgins, L. D., Conroy, M. J., Hounslow, A. M., Jerala, R. *et al.* (2001). Three-dimensional domain swapping in the folded and molten-globule states of cystatins, an amyloid-forming structural superfamily. *EMBO J.* **20**, 4774–4781.
  38. Villanueva, J., Hoshino, M., Katou, H., Kardos, J., Hasegawa, K., Naiki, H. & Goto, Y. (2004). Increase in the conformational flexibility of beta 2-microglobulin upon copper binding: a possible role for copper in dialysis-related amyloidosis. *Protein Sci.* **13**, 797–809.
  39. Kameda, A., Hoshino, M., Higurashi, T., Takahashi, S., Naiki, H. & Goto, Y. (2005). Nuclear magnetic resonance characterization of the refolding intermediate of beta(2)-microglobulin trapped by non-native prolyl peptide bond. *J. Mol. Biol.* **348**, 383–397.
  40. Dobson, C. M. (2006). An accidental breach of a protein's natural defenses. *Nature Struct. Mol. Biol.* **13**, 295–297.
  41. Miranker, A. D. (2005). Structural biology: fibres hinge on swapped domains. *Nature*, **437**, 197–198.
  42. Viles, J. H., Cohen, F. E., Prusiner, S. B., Goodin, D. B., Wright, P. E. & Dyson, H. J. (1999). Copper binding to the prion protein: structural implications of four identical cooperative binding sites. *Proc. Natl Acad. Sci. USA*, **96**, 2042–2047.
  43. Adams, P. L., Stahley, M. R., Kosek, A. B., Wang, J. & Strobel, S. A. (2004). Crystal structure of a self-splicing group I intron with both exons. *Nature*, **430**, 45–50.
  44. Laity, J. H., Lee, B. M. & Wright, P. E. (2001). Zinc finger proteins: new insights into structural and functional diversity. *Cur. Opin. Struct. Biol.* **11**, 39–46.
  45. Cox, C. & Lectka, T. (2000). Synthetic catalysis of amide isomerization. *Acc. Chem. Res.* **33**, 849–858.
  46. Stray, S. J., Ceres, P. & Zlotnick, A. (2004). Zinc ions trigger conformational change and oligomerization of hepatitis B virus capsid protein. *Biochemistry*, **43**, 9989–9998.
  47. Eakin, C. M., Knight, J. D., Morgan, C. J., Gelfand, M. A. & Miranker, A. D. (2002). Formation of a copper specific binding site in non-native states of beta-2-microglobulin. *Biochemistry*, **41**, 10646–10656.

*Edited by C. R. Matthews*

(Received 20 September 2006; received in revised form 9 December 2006; accepted 13 December 2006)  
Available online 19 December 2006